Orientation and Effects of Mastoparan X on Phospholipid Bicelles

Jennifer A. Whiles,* Robert Brasseur,[†] Kerney J. Glover,* Giuseppe Melacini,* Elizabeth A. Komives,* and Regitze R. Vold*

*Department of Chemistry and Biochemistry, University of California San Diego, La Jolla, California 92093 USA; and
[†]Universitaire des Sciences Agronomiques de Gembloux Centre de Biophysique Moléculaire Numérique, B-5030-Gembloux, Belgium

ABSTRACT   Mastoparan X (MPX: INWKGIAAMAKKLL-NH$_2$) belongs to a family of ionophoric peptides found in wasp venom. Upon binding to the membrane, MPX increases the cell's permeability to cations leading to a disruption in the electrolyte balance and cell lysis. This process is thought to occur either through a membrane-thinning mechanism, where the peptide resides on the membrane surface thereby disrupting lipid packing, or through formation of an oligomeric pore. To address this issue, we have used both high-resolution and solid-state ^{2}H NMR techniques to study the structure and orientation of MPX when associated with bicelles. NOESY and chemical shift analysis showed that in bicelles, MPX formed a well-structured amphipathic α-helix. In zwitterionic bicelles, the helical axis was found to rest generally perpendicular to the membrane normal, which could be consistent with the "carpet" mechanism for lytic activity. In anionic bicelles, on the other hand, the helical axis was generally parallel to the membrane normal, which is more consistent with the pore model for lytic activity. In addition, MPX caused significant disruption in lipid packing of the negatively charged phospholipids. Taken together, these results show that MPX associates differently with zwitterionic membranes, where it rests parallel to the surface, compared with negatively charged membranes, where it penetrates longitudinally.

INTRODUCTION

Mastoparan X (MPX: INWKGIAAMAKKLL-NH$_2$) is a 14-residue peptidic toxin found in wasp venom. Mastoparans (MPs) in general have a variety of physiological roles including mast cell degranulation, calmodulin binding (Malencik and Anderson, 1983), G-protein activation (Higashijima et al., 1988), stimulation of phospholipase A$_2$ (Argiolas and Pisano, 1983), and permeabilization of planar bilayers to cations (Okamura et al., 1981). In general, it is thought that lytic peptides destroy membranes either by disrupting lipid packing, termed the carpet mechanism, and/or through formation of an ion channel, termed the barrel stave mechanism (Epand et al., 1995).

Many factors have been found to affect peptide permeabilization of membranes, including lipid composition, ionic strength, and transmembrane potential. MPX partitions differently in vesicles composed of lipids with identical headgroups but different fatty acid chain lengths. Specifically, fluorescence studies revealed steeper association isotherms for MPX in dioleoyl phosphatidylcholine vesicles as compared with palmitoyloleoyl phosphatidylcholine vesicles, and these isotherms were affected differently by increasing salt concentrations (Hellmann and Schwarz, 1998). Similar studies also showed that the association of MPX varied with vesicle size (Hellmann and Schwarz, 1998; Arbuzova and Schwarz, 1999). The presence of certain lipids with negatively charged headgroups, such as phos-

phatidylglycerol, increase the association of MPX with model membranes (de Kroon et al., 1991). Furthermore, MPX induced a higher extent of dye leakage from vesicles doped with anionic lipids (Matsuzaki et al., 1996). The ionic strength has been shown to affect both the partitioning (de Kroon et al., 1991; Schwarz and Blochmann, 1993; Hellmann and Schwarz, 1998) and conductance levels (Mellor and Sansom, 1990) of MPs in lipid bilayers. However, peptides within the MP family have been shown to be affected differently. For example, circular dichroism studies of mastoparan in comparison with MPX showed that the peptide underwent significant conformational changes as a function of NaCl concentration whereas the conformation of MPX was unaffected (Schwarz and Blochmann, 1993). There is also evidence suggesting that a transmembrane potential may be linked to MPX activity (de Kroon et al., 1991). However, other studies indicate that MPX may still be capable of some ionophoric activity in the absence of a potential (Matsuzaki et al., 1996; Arbuzova and Schwarz, 1996, 1999).

Attempts to determine the location of MPX within the membrane have been made using various fluorescence techniques. For example, fluorescence quenching of the MPX tryptophan residue (W3) by 5-doxylstearic acid in dimyristoyl phosphatidylcholine (DMPC) vesicles was more efficient than quenching by 12- or 16-doxylstearic acid. This suggested that the tryptophan rested close to the membrane surface (Fujita et al., 1994). Other experiments showed that the W3 fluorescence emission maximum shifted to a longer wavelength upon titration with large unilamellar vesicles. This wavelength was also compatible with the location of W3 in a semi-hydrophobic environment, again suggesting that MPX rested near the vesicle surface (Matsuzaki et al., 1996). Fluorescence resonance energy transfer experiments

between W3 and NBD-labeled dipalmitoylphosphatidylethanolamine in vesicles showed that MPX did not penetrate into zwitterionic bilayers as deeply as negatively charged bilayers (Arbuzova and Schwarz, 1999). Although these experiments gave considerable information concerning the interaction of MPX with lipids, they could not define the angle of orientation of MPX with respect to a bilayer or reveal the effects of MPX on specific lipids.

Solid-state NMR techniques allow a quantitative measure of the orientation of a molecule with respect to a lipid bilayer. Typically, a ^{15}N-labeled peptide is studied in mechanically aligned lipid bilayers (Cross and Opella, 1994; Bechinger et al., 1998). Using this technique, the 23-residue peptide magainin was found to rest parallel to the lipid-solvent interface of palmitoyloleoyl phosphatidylcholine bilayers with its helical axis perpendicular to the membrane normal (Bechinger et al., 1992) whereas 20-residue alamethicin inserted into DMPC bilayers with its helical axis parallel to the membrane normal (North et al., 1995). Solid-state deuterium NMR has also been used to study the orientation of transmembrane peptides in lipid bilayers (Jones et al., 1998). Deuterium NMR has the advantage that the quadrupolar interaction is so strong that dipolar and chemical shift interactions can be neglected (Davis, 1983).

Solid-state deuterium NMR can be used to study the orientation of peptides and proteins in oriented bilayered micelles, or bicelles. A bicelle is a lipid aggregate composed of long- and short-chain phospholipids. Due to the magnetic susceptibility of the methylene chains of the long-chain phospholipid, bicelles spontaneously align with their normals generally perpendicular to the magnetic field at $q > 2$ (ratio of long-chain to short-chain phospholipid) and $c_L \approx$ 15–25% (total phospholipid concentration) (Sanders and Schwonek, 1992). In this phase, the bicelles are discoidal with the lipid pools segregated into a planar bilayer of long-chain phospholipid surrounded by a rim of short-chain phospholipid that protects the fatty acyl chains from exposure to water (Ram and Prestegard, 1988; Sanders et al., 1994; Vold et al., 1997). Both peptide and lipid orientation can be extracted from the solid-state NMR spectra of such aligned bicelle samples (Sanders and Prestegard, 1990; Sanders and Landis, 1995; Sanders et al., 1994; Howard and Opella, 1996; Losonczi and Prestegard, 1998; Struppe et al., 1998). In this study, we have incorporated MPX into bicelles and have used deuterium solid-state NMR to determine its motionally averaged angle of orientation as well as its effects on lipid packing.

Bicelles, unlike mechanically aligned bilayers, also permit high-resolution NMR structural studies in a phase of similar composition. At $q < 1$ and $c_L \approx$ 10–15%, bicelles form an unaligned phase that is suitable for high-resolution NMR studies (Vold et al., 1997). Work in our lab has shown that these bicelles are also discoidal and the lipid pools remain segregated as they are in the aligned phase (manuscript in preparation). Advantageously, these small bicelles will permit high-resolution NMR structures of membrane-associated peptides to be determined in a flat planar bilayer. Detergent micelles are commonly used for NMR structural studies of membrane peptides; however, some MPs have been shown to exhibit biological activity that differed dramatically in the presence of detergent (Mellor and Sansom, 1990). Because bicelles are prepared entirely from phospholipids, they may provide a more biochemically friendly environment for MPX. Bicelles can also be prepared with mixtures of zwitterionic and anionic phospholipids, which provide more versatility in membrane composition than can be achieved with detergents alone (Struppe et al., 2000). In particular, we were able to incorporate dimyristoyl phosphatidylserine, one of the most abundant negatively charged phospholipids in eukaryotic cell membranes, into our bicelle samples.

Our results showed that MPX forms a well-structured amphipathic helix when associated with both zwitterionic and anionic bicelles. However, the orientation of the helical axis varied with bicelle composition. In zwitterionic bicelles, the helical axis was found to rest generally perpendicular (84° or 75°) to the membrane normal, which could be consistent with the carpet mechanism for lytic activity. In anionic bicelles, on the other hand, the helical axis was generally parallel to the membrane normal (17°), which is more consistent with the pore model for lytic activity.

MATERIALS AND METHODS

Materials

Fluorenyl-methoxycarbonyl (FMOC) and pentafluorophenol amino acids and 1-hydroxy-7-azabenzotriazole were purchased from PE Biosystems (Foster City, CA). Deuterium-depleted water, deuterium oxide, and L-alanine-(3,3,3-d_3, 99%) were obtained from Cambridge Isotope Labs (Andover, MA). All other synthesis reagents were obtained from Fisher Scientific (Pittsburgh, PA), Aldrich Chemical Co. (Milwaukee, WI), or VWR Scientific (Los Angeles, CA) and were used as received. Dimyristoyl-d_{54} phosphatidylcholine (DMPC-d_{54}), dimyristoyl-d_{54} phosphatidylserine (DMPS-d_{54}), dihexanoyl-d_{22} phosphatidylcholine (DHPC-d_{22}), and their nondeuterated counterparts were obtained from Avanti Polar Lipids (Alabaster, AL) and used without further purification.

Peptide preparation

MPX and its isotopically labeled counterparts (MPX: INWKGIAAMAKKLL-NH$_2$; MPX-A7$_{d3}$: INWKGI(d_3-A)AMAKKLL-NH$_2$; MPX-A8$_{d3}$: INWKGIA(d_3-A)MAKKLL-NH$_2$; MPX-A10$_{d3}$: INWKGIAAM(d_3-A)KKLL-NH$_2$; MPX-^{15}N: INWK(^{15}N-G)IA(^{15}N-A)M(^{15}N-A)KKLL-NH$_2$) were synthesized using FMOC chemistry on a MilliGen 9050 solid-state peptide synthesizer. The peptide was purified by reverse-phase high-performance liquid chromatography using a Deltapak C18 radial compression column (Waters, Milford, MA) and a standard linear gradient from 0.1% trifluoroacetic acid to acetonitrile. The purity of the peptide was verified by mass spectrometry and one-dimensional (1D) NMR. Lyophilized peptide was resuspended in ^{2}H-depleted water and assayed spectrophotometrically to determine the concentration (absorbance at 280 nm using a molar absorptivity 5690 M/cm (Edelhoch, 1967)).

Sample preparation

Samples of MPX in bicelles were prepared by suspending the appropriate amount of peptide stock solution and long-chain phospholipid (DMPC for zwitterionic bicelles and 3:1 DMPC:DMPS for negatively charged bicelles) in ^{2}H-depleted water for solid-state NMR samples and 80:20 $H_2O:D_2O$ for high-resolution NMR studies. Phospholipid with deuterated fatty-acyl chains was used in all samples for high-resolution NMR experiments. The samples were vortexed and briefly centrifuged (low speed at room temperature), and the pellet was then resuspended with vortexing. Repeating this cycle two to three times resulted in a uniform suspension of peptide and long-chain lipid and allowed for bicelle formation once the short-chain lipid was added. DHPC from a stock solution (in ^{2}H-depleted water) was added to the mixture to achieve $q = 3.5$ and $c_L = 20\%$ (w/v) for solid-state samples and $q = 0.4$ and $c_L = 15\%$ (w/v) for high-resolution samples. The samples were vortexed and centrifuged until clear to ensure homogeneous mixing. No pelleted lipid was separated from the sample after each centrifugation step; it was resuspended with the next cycle of vortexing and occasional heating until no pellet formed upon further centrifugation. In viscous solid-state samples, rapid cooling in liquid N_2 facilitated mixing and subsequent formation of a uniform suspension. The final pH was adjusted to 5.4 for the zwitterionic bicelle samples and 5.8 for the negatively charged bicelle samples; this was done to minimize amide exchange during the proton NMR experiments. The molar ratio of MPX to total long-chain lipid (R) was 1:40 in all high-resolution NMR samples and varied from 1:40 (lowest peptide concentration) to 1:10 (highest peptide concentration) in the solid-state NMR samples.

One- and two-dimensional homonuclear NMR

All spectra were recorded at 37°C on a Bruker DRX 600-MHz spectrometer equipped with a 5-mm TXI probe. One-dimensional ^{1}H spectra were recorded using the WATERGATE pulse sequence to suppress the water signal (Piotto et al., 1992). One-dimensional WATERGATE spectra preceded by the Carr-Purcell-Meiboom-Gill sequence with different repetition rates (CPMG-WATERGATE) were also acquired to assess line broadening due to chemical exchange (van Tilborg et al., 1999). These experiments had repetition delays for π pulses of 15.24 μs, 241 μs, and 2.5 ms. Standard 2D TOCSY and NOESY spectra were acquired with water suppression again achieved through the WATERGATE sequence. Quadrature phase detection in the indirectly detected dimension was obtained via time proportional phase incrementation (Marion and Wüthrich, 1983). The TOCSY had a 60-ms MLEV-17 spin lock and the NOESY had a 150-ms mixing time. The signals were averaged over at least 64 transients.

Typical relaxation experiments were performed on MPX-^{15}N at 37°C on the 600-MHz spectrometer using pulse trains for measuring the longitudinal (R_1) and transverse (R_2) relaxation rates as well as the heteronuclear NOE ([^{1}H]-^{15}N NOE) modified from Farrow et al. (1994). R_1 was measured for the amides of G5, A8, and A10 of MPX-^{15}N in zwitterionic bicelles, negatively charged bicelles, and negatively charged bicelles with 150 mM KCl from spectra recorded with the following relaxation delay times: $T = 40, 100, 200, 300, 400, 500, 600, 800, 1000,$ and 1280 ms. The corresponding values for R_2 were measured from spectra recorded with the following relaxation delay times: for MPX-^{15}N in neutral bicelles, $T = 12, 24, 36, 60, 80, 96, 120, 240,$ and 320 ms; for MPX-^{15}N in negatively charged bicelles, $T = 12, 24, 36, 48, 64, 80, 96,$ and 120 ms; and for MPX-^{15}N in negatively charged bicelles with 150 mM KCl, $T = 12, 24, 36, 60, 80, 96, 120,$ and 180 ms. All NMR experiments were processed with the MSI Felix 97.0 software package (San Diego, CA).

Relaxation rate constants and heteronuclear NOEs were calculated from cross-peak heights in the ^{1}H-^{15}N correlation spectra. The program Curvefit (Palmer, 1998a) was used to extract the rate constants and their standard deviations from the relaxation data, and Lipari-Szabo Formalism (Lipari and Szabo, 1982a,b) was then used to extract the overall isotropic corre-

lation time τ_m and the generalized order parameter S^2 from the relaxation data using the program Modelfree (Palmer, 1998b).

Solid-state ^{2}H NMR

Deuterium quadrupole echo spectra (Davis et al., 1976) were acquired at either 38.4 or 55.3 MHz. The 38.4-MHz GN500 spectrometer was controlled by a Tecmag LIBRA unit interfaced to an ENI LPI-10 rf amplifier and a 5.9 T Oxford Instruments magnet. Spectra acquired at 38.4 MHz were processed using the Felix 2.1 software package (MSI, San Diego, CA). The 55.3-MHz Chemagnetics CMX-250/360 spectrometer was controlled by a Sun SPARCstation 5 equipped with the Spinsight 3.0 software package (Chemagnetics, Fort Collins, CO) interfaced to an ENI LPI-10 rf amplifier and an 8.5 T Oxford Instruments magnet. The sample temperature in our home-built probes was maintained at 37°C or 40°C with a LakeShore 91C controller. A standard quadrupole echo sequence, $\pi/2$-τ-$\pi/2$-τ_1-acq, was used with an acquisition of at least 512 transients with 4096 data points and a 1.2-s repetition time when observing deuterated lipid and 122,880 transients with 16,384 data points and a 0.9-s repetition time when observing the labeled peptide. Parameters common in both types of experiments were $\tau = 50.0$ μs, $\tau_1 = 35.0$ μs, a $\pi/2$ pulse length of 2.1 μs, and a spectral width of 500.0 kHz to facilitate location of the echo maximum. Data processing included fractional left shifting, zero filling, and multiplication by an exponential (500-Hz line broadening) of the second half of the quadrupole echo before Fourier transformation.

Simulations

A hypermatrix procedure (Brasseur, 1990), derived from that used to surround a drug with lipids (Brasseur et al., 1987) was applied to an α-helical model of MPX energy minimized taking into account the properties of an interface in the presence of an interface (Brasseur, 1990, 1991; Brasseur et al., 1992; Lins and Brasseur, 1995; Nelder and Mean, 1965). Ten different starting models of MPX with different orientations at the interface all gave the same results. In this procedure, the position of the peptide was frozen and a lipid molecule was moved along and around the peptide (2880 positions were tested representing different rotations and translations). For each position, the energy of interaction (van der Waals, electrostatic, torsional, and hydrophobic interactions) was calculated and the energies of all the positions were stored in a hypermatrix. The position of the first lipid was the lowest-energy complex; a second molecule was inserted as the next energetically favorable position in the hypermatrix, taking into account the presence of the first lipid. For the next lipids, the same process was repeated until the peptide was completely surrounded with lipids.

Determination of order parameters

Determination of deuterated phospholipid order parameters

The observed quadrupolar splitting (Δ) for a deuteron in a molecule associated with a bicelle depends on the average order (S_{CD}) of the C—D bond vector with respect to the magnetic field (Seelig, 1977):

$$\Delta = \left(\frac{3}{2}e^2Qq/h\right)S_{CD}, \tag{1}$$

where, e^2Qq/h is the quadrupolar coupling constant ($\sim$168 kHz for an alkyl C—D bond (Seelig, 1977). S_{CD} is described by an order matrix and in the case of uniaxially symmetric motion can be reduced to the principal order parameter S_{zz} (Losonczi and Prestegard, 1998). S_{zz} can then be expressed as a product of order parameters (S_i), each of which describes the average

orientation (β_i) of the C—D bond vector within a defined coordinate system:

$$S_i = \langle 1/2(3 \cos^2\beta_i - 1) \rangle \tag{2}$$

As determined previously (Prosser et al., 1998), the relevant order parameters S_i necessary to fully describe the observed quadrupolar splitting of a deuterated phospholipid in a bicelle ($\Delta_{\mathrm{BIC}}^{\mathrm{L}}$) are shown in Eq. 3:

$$\Delta_{\mathrm{BIC}}^{\mathrm{L}} = (252 \text{ kHz})S_{\mathrm{pm}}S_{\mathrm{mn}}S_{\mathrm{nN}}S_{\mathrm{Nl}} \tag{3}$$

As mentioned earlier, bicelles align with their normals perpendicular to $\mathbf{B_o}$ ($\beta_{\mathrm{IN}} = 90°$) resulting in a bicelle order parameter, S_{Nl}, of 1/2. S_{pm} is the individual lipid reorientational order parameter, and studies of lipids in bilayers have determined its value to be ~0.25 (Bloom et al., 1991). The uniaxial rotation of the lipid about its long molecular axis results in a net C—D bond vector (**pm**) that is parallel to **m** (Fig. 1 *A*). Bicelle spinning about its normal results in an angle β_{mn} between **pm** and **n** of $\sim0°$ and consequently a S_{mn} of 1 using Eq. 2 (Vold and Prosser, 1996; Prosser et al., 1998). The new net C—D bond vector (**mn**) is therefore parallel to **n**.

In an ideal system, all bicelles would align with their normals exactly perpendicular to the magnetic field. However, there is a significant degree of fast wobble (S_{nN}) of **mn** about **N**, which yields a final C—D bond vector that is parallel to the average bicelle normal (Prosser et al., 1998). S_{nN} can be approximated by taking the ratio of the quadrupolar splitting of the plateau deuterons (those closest to the DMPC-d_{54} headgroup and with the largest quadrupolar splitting) in a bicelle versus that of a multilamellar vesicle (MLV). If the reasonable assumption is made that S_{pm} (lipid order) is the same in a MLV as in a bicelle, the observed quadrupolar splitting for DMPC-d_{54} can be expressed similarly to Eq. 3:

$$\Delta_{\mathrm{MLV}}^{\mathrm{L}} = (252 \text{ kHz})\left(\frac{1}{2}\right)S_{\mathrm{pm}}, \tag{4}$$

where a factor of 1/2 arises because we are measuring at the 90° edge of the powder pattern. Dividing Eq. 3 by Eq. 4 allows S_{nN} to be expressed as

$$S_{\mathrm{nN}} = \Delta_{\mathrm{BIC}}^{\mathrm{L}}/\Delta_{\mathrm{MLV}}^{\mathrm{L}}. \tag{5}$$

Determination of peptide order parameters

The observed quadrupolar splitting (Δ^{P}) of a deuteron in a peptide associated with a bicelle can be described by Eq. 1. Again, S_{CD} can be represented as a product of order parameters S_i arising from both peptide and bicelle order. To obtain an accurate description of the orientation of a peptide with respect to the bicelle surface, all order parameters, which represent motion on a time scale that is short compared with the time scale of the measured quadrupolar interaction, must be accounted for. Our discussion of peptide order is based on a methodology presented by Jones et al. (1998), which we found integrated well with the framework we use to describe bicelle order (Jones et al., 1998; Kovacs and Cross, 1997). As with the analysis of the lipid splitting, the quadrupolar splitting for a deuterated peptide (Δ^{P}) can be expressed as

$$\Delta^{\mathrm{P}} = (252 \text{ kHz})S_{\mathrm{mr}}S_{\mathrm{rp}}S_{\mathrm{pw}}S_{\alpha\mathrm{n}}S_{\mathrm{nN}}S_{\mathrm{Nl}}. \tag{6}$$

The first-order parameter we must consider is S_{mr}, which accounts for fast rotation of the alanine methyl group. Based on the geometry of an alanine residue, this motion results in a value of 1/3 for S_{mr} and a resultant C—D bond vector **mr** along the C^α—C^β bond. Because the methyl group is attached directly to the peptide backbone, the next possible order parameter is S_{rp}, arising from fast uniaxially symmetric rotation about the helical axis (we will experimentally show that MPX is an α-helix). A model of MPX constructed in Insight II (MSI, San Diego, CA) shows that the angle between **mr** and the helical axis is 56°. An order parameter describing this rotation would subsequently collapse the quadrupolar splitting to ~0 kHz.
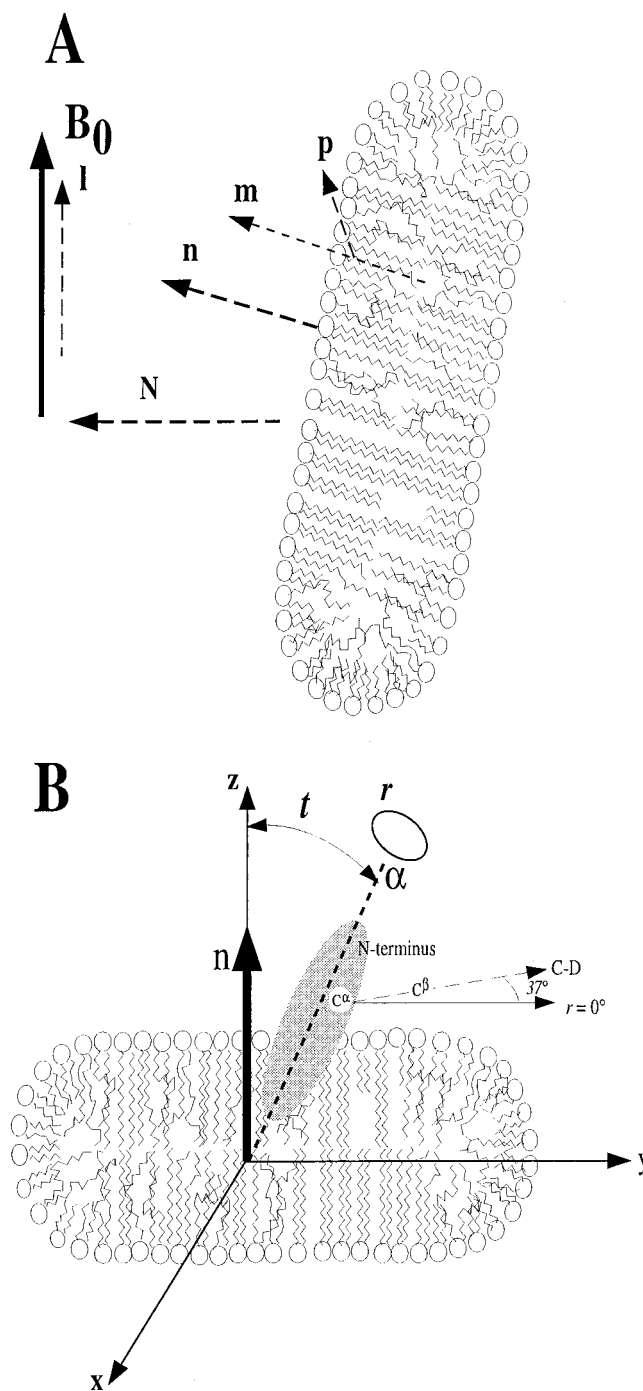

FIGURE 1 (*A*) Representation of the important axes involved in determination of the order parameters responsible for scaling the quadrupolar splitting of a fatty acid perdeuterated phospholipid in a bicelle. In this schematic, p represents the original C—D bond vector for a deuterated methylene group, m is the molecular axis of the phospholipid, n is the bicelle normal, N is the net bicelle normal (arising from alignment of the bicelles in the magnetic field), and l is the direction of the magnetic field in the laboratory frame. (*B*) Representation of the coordinate system used to define the tilt (*t*) and rotation (*r*) of the MPX α-helix with respect to the bicelle normal.

FIGURE 2 One-dimensional ^{1}H spectra of MPX in water (1.5 mM peptide; *A*), zwitterionic bicelles (*R* = 1:40; *B*), and negatively charged bicelles (*R* = 1:40; *C*). *R* = ratio of peptide to total long-chain phospholipid. All spectra were recorded at 37°C and the residual water line was referenced to 4.623 ppm (Wishart et al., 1995). The peptide spectra in water and zwitterionic bicelles were acquired at pH 5.4 and the peptide spectrum in negatively charged bicelles was acquired at pH 5.8.
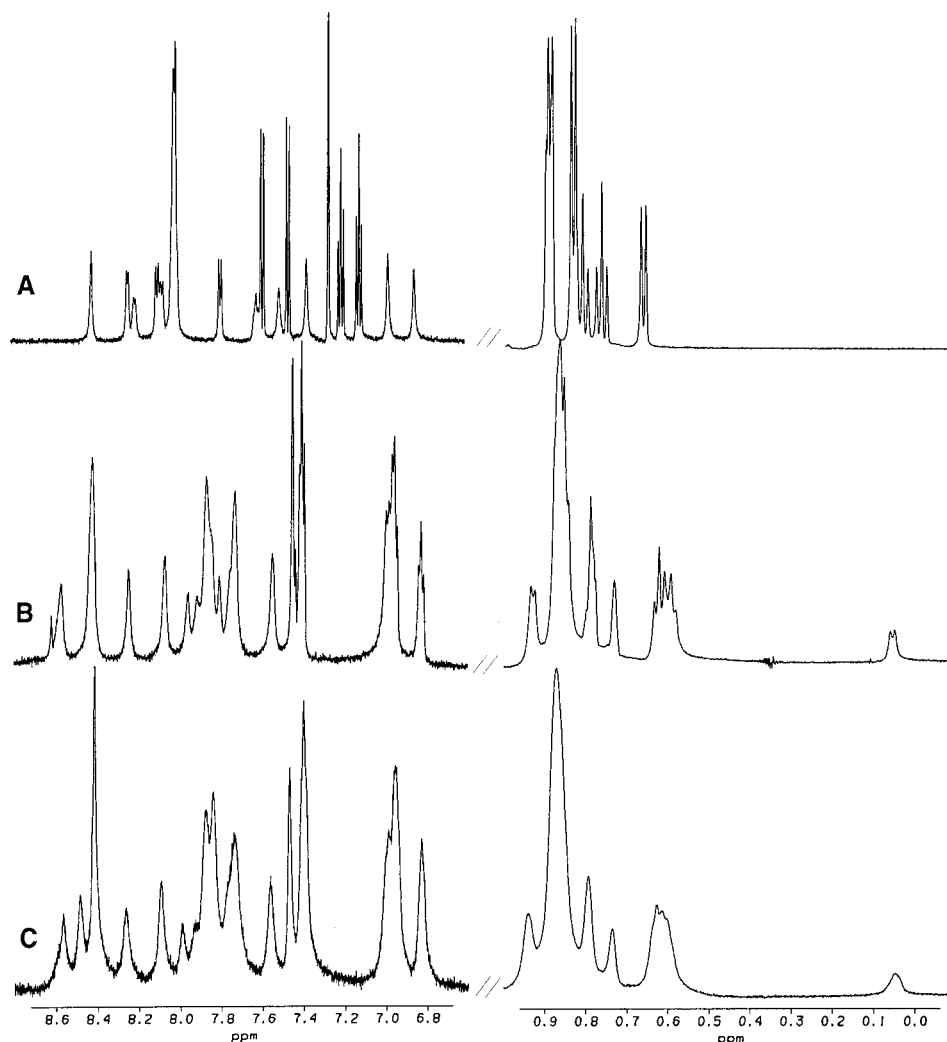
Overall, the splittings we observe are greater than those expected for fast helical rotation, and because MPX is an amphipathic α-helix, fast rotation about the helical axis would be energetically unfavorable. Therefore, we assign a value of 1 to S_{rp}, but note that partial rotations about the helical axis could still result in a small degree of motional averaging. The remaining peptide order parameter we must consider, S_{pw}, reflects conformational instability and helix wobble about the major and/or minor axis (which could result in motional averaging of the peptide tilt angle with respect to the bicelle normal). This parameter will be determined experimentally by analysis of the relaxation rate constants and heteronuclear NOEs obtained using high-resolution solution NMR techniques.

Similar to the order parameter S_{mn} for deuterated lipids in bicelles, uniaxial bicellar motion about its normal will result in an order parameter $S_{\alpha n}$. If we assume that slight rolls about the helical axis and overall peptide wobble are minimal (the latter of which is supported by the dynamics studies) then the orientation of MPX with respect to the bicelle normal can be considered to be fixed. The value of $S_{\alpha n}$ will depend on the average tilt angle (*t*) of the peptide helical axis with respect to **n** (assuming that the majority of MPX interacts with the planar region of the bicelle, which our data supports). Because our solution-state NMR structure and dynamics will show that MPX forms a rigid amphipathic α-helix, particularly around the regions of our deuterium labels in the solid-state work, we would expect that if there were no preference for which face of the helix associated with the membrane, then all of the alanine residues would have the

same deuterium spectra for a particular tilt angle. However, our observations of different quadrupolar splittings for the three labeled alanines, indicates preferential binding of one face of the helix to the bicelle. Therefore, we must account for a fixed degree of rotation (*r*) about the helical axis (α). As described in Jones et al., we established a coordinate system where $r = 0°$ when the C^α of A7 is directed along the positive y axis and counterclockwise rotation about α is positive (Fig. 1 *B*) (Jones et al., 1998). The cosine of the angle between the C—D bond vector and the membrane normal can then be expressed in terms of *t* and *r*:

$$\text{for A7, } \cos \beta_{\alpha n} = -\sin 56° \cos (r)\sin t + \cos 56° \cos t \tag{7}$$

$$\text{for A8, } \cos \beta_{\alpha n} = -\sin 56° \cos(r + 260°)\sin t + \cos 56° \cos t \tag{8}$$

$$\text{for A10, } \cos \beta_{\alpha n} = -\sin 56° \cos(r + 60°)\sin t + \cos 56° \cos t \tag{9}$$

Eqs. 7–9 will result in varying $S_{\alpha n}$ for the different labeled peptides. (Determination of the actual rotation angle was corrected for the 37° difference between the defined coordinate axis 0 position (along the y axis)
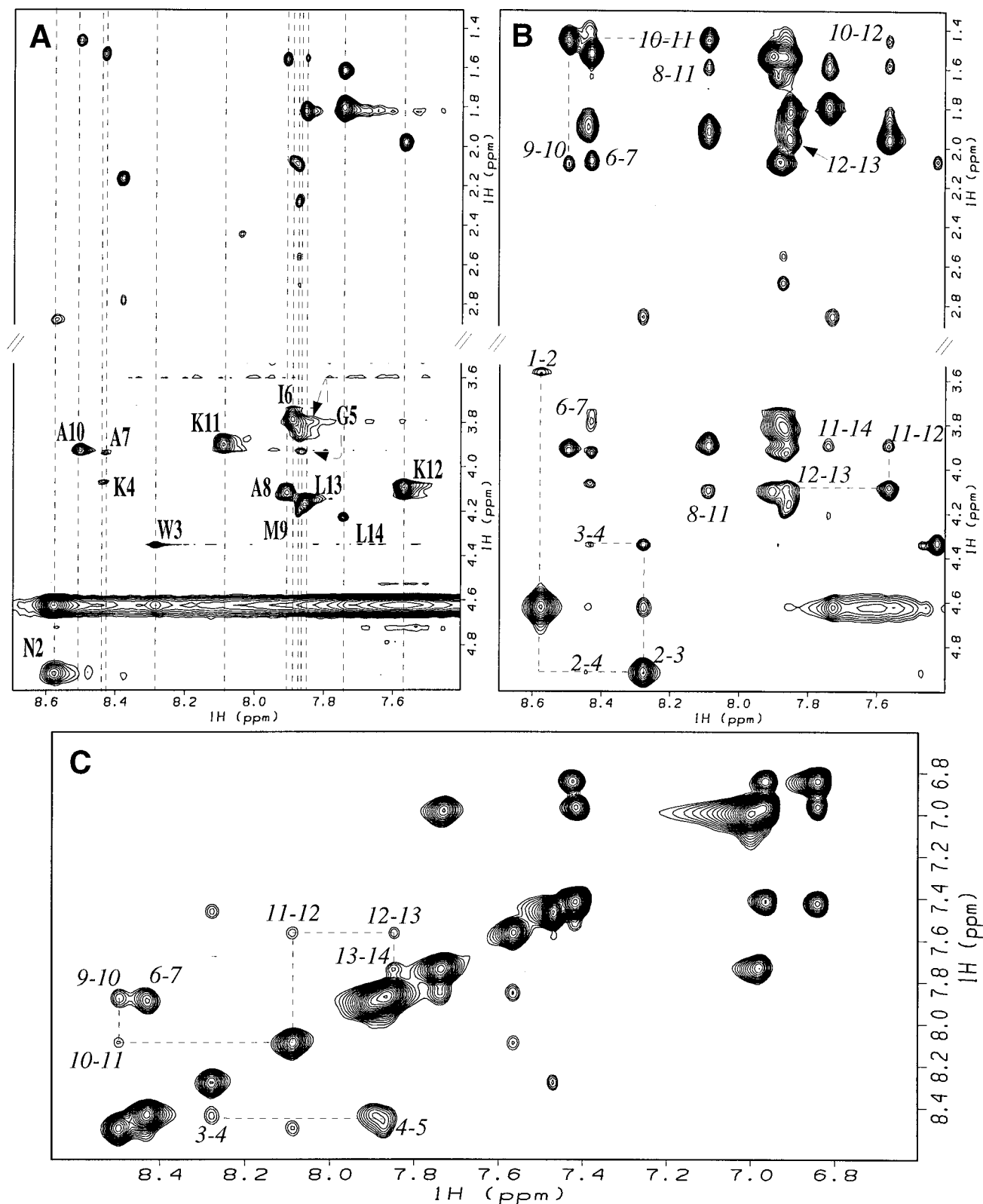
FIGURE 3 Two-dimensional homonuclear spectra for MPX in zwitterionic bicelles with 150 mM KCl. (a) The TOCSY spectrum; (*B*) the H^N-H^α region of the NOESY spectrum; (*C*) the H^N-H^N region of the NOESY spectrum. The TOCSY spectrum was recorded with a 60-ms spin locking time and the NOESY mixing time was 150 ms. Both spectra were acquired at 37°C and pH 5.4, and the residual water line was referenced to 4.623 ppm (Wishart et al., 1995).

A

B
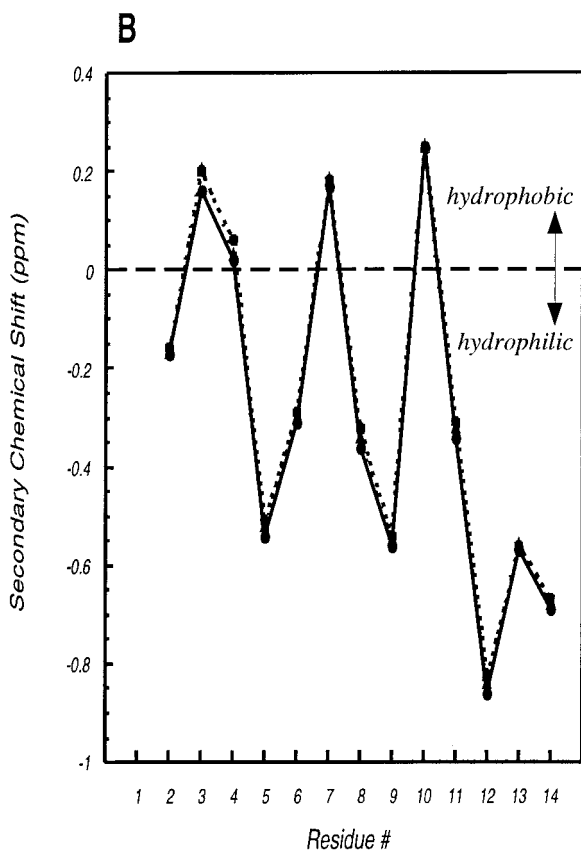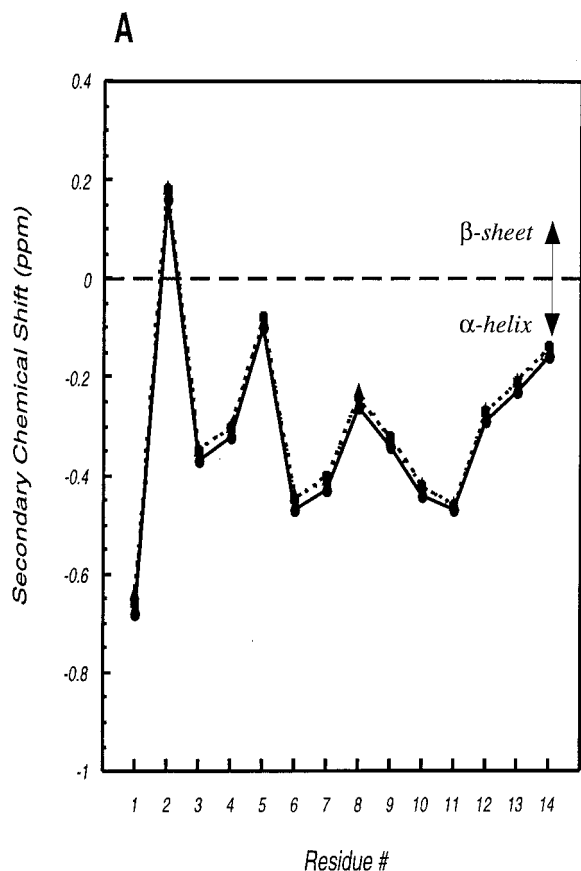
TABLE 1 ^{1}H chemical shifts of MPX in bicellar solution with 150 mM KCl at pH 5.4 and 37°C

Residue	Chemical shift (ppm)		
	NH	C^αH	C^βH
Ile^1	—	3.59	1.49
Asn^2	8.58	4.93	2.89, 3.05
Trp^3	8.29	4.35	3.30, 3.06
Lys^4	8.44	4.06	1.93, 1.87
Gly^5	7.87	3.82, 3.94	
Ile^6	7.89	3.79	2.08
Ala^7	8.43	3.94	1.53
Ala^8	7.91	4.12	1.56
Met^9	7.87	4.19	2.09
Ala^{10}	8.50	3.93	1.46
Lys^{11}	8.09	3.90	1.94, 1.72
Lys^{12}	7.57	4.09	1.98, 1.72
Leu^{13}	7.86	4.17	1.84, 1.79
Leu^{14}	7.74	4.23	1.79, 1.62

The chemical shifts were referenced to water at 4.623 ppm (*Wishart et al., 1995*). The experimental uncertainty is approximately ±0.01 ppm.

and the C—D bond vector along the C^α—C^β bond (Fig. 1 *B*).) Having accounted for variations in $S_{\alpha n}$ due to residue position, the resulting C—D bond vector (**nN**) is parallel to the bicelle normal. The remaining order parameters, S_{nN} and S_{Nl}, are the same as were determined for a deuterated phospholipid in a bicelle. Substitution of these order parameters as well as the quadrupolar coupling constant into Eq. 6 leads to

$$\Delta^P = (42 \text{ kHz})S_{pw}S_{\alpha n}S_{nN}, \tag{10}$$

where $S_{\alpha n}$ varies with the position of the alanine label.

A C++ computer program allowed computation of the tilt angles (varied in 1° intervals from 0° to 90°) and the rotation angles (varied in 1° increments from 0° to 360°) that were consistent with the quadrupolar splitting of all three alanine labels. The program then ranked all possible tilt and rotation angle combinations based on how far the individual and average quadrupolar splittings varied from the theoretical values for a particular tilt and rotation.

RESULTS AND DISCUSSION

One-dimensional NMR

To initially explore the effects of lipid environment on the structure of MPX, 1D ^{1}H spectra were collected under five different sample conditions: MPX in water (MPXWAT), MPX in zwitterionic bicelles (MPXZB), MPX in zwitterionic bicelles with 150 mM KCl (MPXZBKCL), MPX in negatively charged bicelles (MPXNB), and MPX in negatively charged bicelles with 150 mM KCl (MPXNBKCL).

FIGURE 4 Plots of secondary chemical shifts as a function of residue number for H$^\alpha$ (*A*) and H^N (*B*) at 37°C for MPX in zwitterionic bicelles (*solid line*), zwitterionic bicelles with 150 mM KCl (*dotted line*), and negatively charged bicelles with 150 mM KCl (*dashed line*). The secondary chemical shift was calculated by subtracting the random coil value (Wüthrich, 1986) from the experimental value. The zwitterionic bicelle samples were at pH 5.4, and the negatively charged bicelle samples were at pH 5.8.
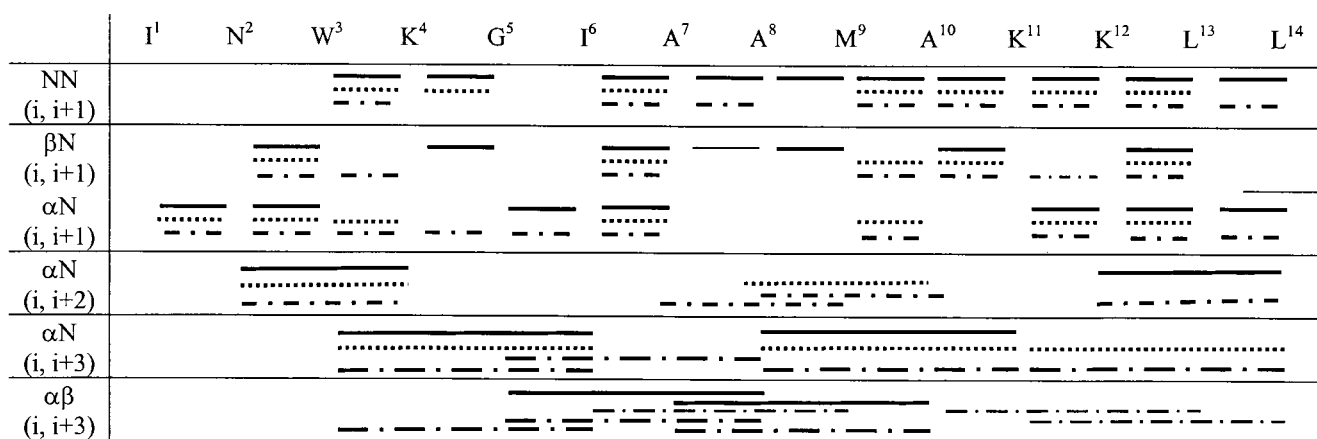
	I[1]	N[2]	W[3]	K[4]	G[5]	I[6]	A[7]	A[8]	M[9]	A[10]	K[11]	K[12]	L[13]	L[14]
NN (i, i+1)														
βN (i, i+1)														
αN (i, i+1)														
αN (i, i+2)														
αN (i, i+3)														
αβ (i, i+3)														

FIGURE 5   NOE connectivites observed in MPX for peptide bound to zwitterionic bicelles (*solid lines*), zwitterionic bicelles with 150 mM KCl (*dotted lines*), and negatively charged bicelles with 150 mM KCl (*dashed/dotted lines*). NOESY spectra were recorded at 37°C with a 150-ms mixing time. The residual water line was referenced to 4.623 ppm (Wishart et al., 1995). The zwitterionic bicelle samples had pH 5.4, and the negatively charged bicelle samples had pH 5.8. Thin lines represent ambiguous NOE cross-peaks that were difficult to interpret due to residual signal from the phospholipids.

As shown in the representative spectra in Fig. 2, the peptide signals had greater chemical shift dispersion in the bicelle samples (Fig. 2, *B* and *C*) than in water alone (Fig. 2 *A*), indicating that the peptide assumed secondary structure in the presence of bicelles. A characteristic upfield peak located near 0.1 ppm, later assigned to the methyl group of I1, appeared in all bicelle samples but was absent in the MPX-WAT spectrum. The I1 methyl group would become ring-shifted upfield by W3 when the peptide formed the helical structure later suggested by the 2D homonuclear NMR experiments.

Compared with the MPX spectrum in water, the line-widths of MPX in bicelles were significantly larger. This line broadening could be due to the presence of a peptide-bicelle interaction and/or chemical exchange. The second possibility was addressed through the acquisition of CPMG-WATERGATE spectra for MPXZB and MPXNB. As the delay period between π pulses (15.24 μs, 241 μs, and 2.5 ms) in the CPMG pulse sequence was increased, no significant change in intensity was observed for either sample (data not shown), indicating that MPX was not undergoing chemical exchange on the millisecond time scale. There-

fore, the line broadening observed for MPX in bicelles compared with in water is likely due to a peptide-bicelle interaction.

Two-dimensional homonuclear NMR

To determine the structure of MPX when associated with bicelles, TOCSY and NOESY spectra were acquired under the same conditions as the 1D spectra. TOCSY and NOESY spectra for MPXZBKCL are shown in Fig. 3, and the corresponding resonance assignments are summarized in Table 1. Resonances for all amino acids were present and could be assigned. The two-dimensional spectra for all samples with MPX in bicelles were similar to that for MPXZBKCL with the exception of MPXNB, which had poor linewidths and therefore could not be assigned. However, the NOESY spectrum for MPXNB was very similar to the NOESY spectra of MPX in the other bicelle samples, suggesting that the peptide also maintained the same general secondary structure in negatively charged bicelles. The addition of 150 mM KCl to the sample of MPX in negatively

TABLE 2   Relaxation rate constants and heteronuclear NOEs from MPX-^{15}N NMR relaxation experiments

Sample	Residue	R_1	R_2	[^{1}H]-^{15}N NOE	Average τ_m (ns)	Average S^2
MPXNB	G5	1.38 ± 0.04	10.95 ± 0.05	0.628 ± 0.006	8.01 ± 0.05	0.929 ± 0.006
	A8	1.30 ± 0.03	11.08 ± 0.04	0.626 ± 0.003		
	A10	1.33 ± 0.03	10.96 ± 0.04	0.622 ± 0.003		
MPXAB	G5	1.262 ± 0.004	14.86 ± 0.08	0.67 ± 0.03	10.622 ± 0.006	0.97 ± 0.02
	A8	1.197 ± 0.003	14.95 ± 0.06	0.64 ± 0.01		
	A10	1.269 ± 0.003	14.93 ± 0.006	0.62 ± 0.01		
MPXABKCL	G5	1.357 ± 0.002	11.76 ± 0.09	0.64 ± 0.01	8.98 ± 0.02	0.90 ± 0.03
	A8	1.282 ± 0.001	11.50 ± 0.07	0.65 ± 0.01		
	A10	1.377 ± 0.001	12.11 ± 0.07	0.64 ± 0.01		

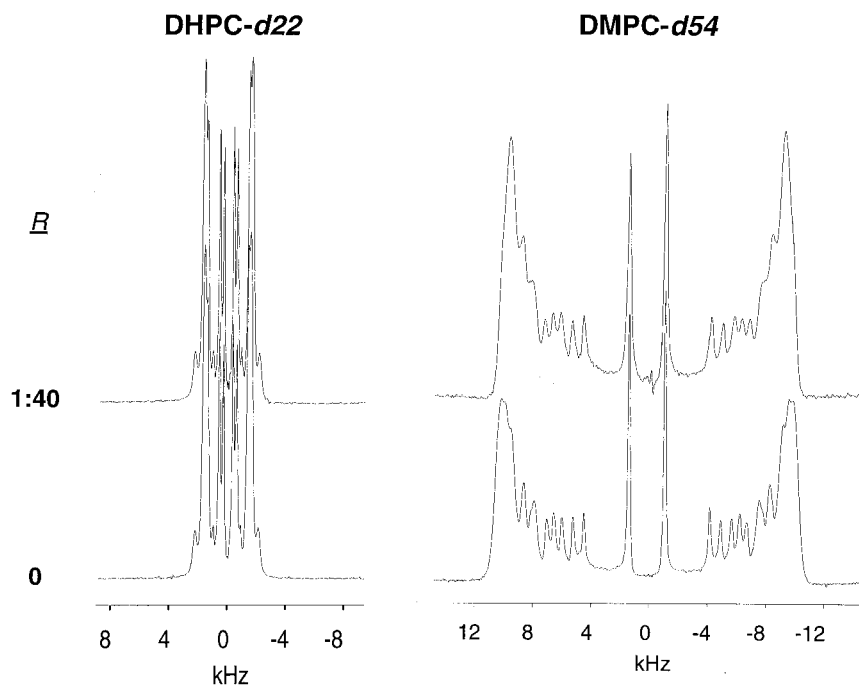**DHPC-*d22***   **DMPC-*d54***

FIGURE 6 Effect of MPX on quadrupolar splittings of perdeuterated phospholipids in zwitterionic bicelles. DHPC-d_{22} and DMPC-d_{54} spectra were recorded at 55.3 MHz at 40°C and pH 5.4. R = ratio of peptide to total long-chain phospholipid.

charged bicelles sample (MPXNBKCL) resulted in a TOCSY spectrum similar to those observed for the peptide in zwitterionic bicelles. Because the addition of salt did not change the MPX spectrum in zwitterionic bicelles, the salt effect on the spectrum for MPX in negatively charged bicelles is not due to a structural change but instead to a modulation of the peptide-bicelle interaction, most likely through electrostatic screening. Later experiments in this study further support this.

MPX associated with bicelles is α-helical as determined by both chemical shift and NOE connectivity analysis. Fig. 4 shows plots of the secondary chemical shifts for the H$^{\alpha}$ (Fig. 4 *A*) and H^{N} (Fig. 4 *B*), calculated by subtracting the random coil chemical shift (Wüthrich, 1986) from the experimental value, as a function of residue number. The negative secondary chemical shifts of the H$^{\alpha}$ (Szilagyi and Jardetzky, 1989) coupled with the NOE connectivites throughout the sequence, shown in Fig. 5, indicate that residues 3–14 of MPX assume an α-helical configuration in the presence of bicelles under all conditions studied. NOEs characteristic of α-helices, αN($i, i + 1$), αN($i, i + 2$), αN($i, i + 3$), and $\alpha\beta$($i, i + 3$) are seen throughout the sequence, including the regions of our isotopic labels. In addition, the ring-shifted I1 methyl group shows that it is held in close proximity to W3, which indicates a high degree of structure at the N-terminus. These structural results agree well with previous studies of MPX in different membrane mimetic systems (Higashijima et al., 1983, 1984; Wakamatsu et al., 1992; Seigneuret and Levy, 1995; Kusunoki et al., 1998). The H^{N} secondary chemical shifts (Fig. 4 *B*) were found to have a three- to four-residue periodicity with the more

hydrophobic residues generally shifting downfield and the more hydrophilic residues generally shifting upfield. Similar results have been observed previously for amphipathic α-helices (Kuntz et al., 1991; Zhou et al., 1992). Reymond et al. (1997) showed that when opportunities for hydrogen bonding between the helix and water are reduced, the downfield shift of amide protons on the hydrophobic face of helices was intensified. Similarly, this periodicity, along with a blue-shifted W3 fluorescence spectrum (unpublished results), suggests that in our system, the MPX α-helix is amphipathic with its hydrophobic face interacting with the lipid bilayer (Vold et al., 1997). However, the interaction of the hydrophobic face of MPX with the bicelle could be satisfied by either the peptide resting parallel to the membrane surface or inserted in the form of a pore.

MPX dynamics

To determine the flexibility and wobble of the MPX helix, R_1, R_2, and heteronuclear NOEs were measured for MPX-^{15}N-containing isotopic labels at G5, A8, and A10. The results from these experiments as well as the resulting τ_m

TABLE 3 **Quadrupolar splittings for MPX in bicelles (kHz)**

Label Position	Zwitterionic bicelles	Anionic bicelles
A7	Not resolvable	6.3
A8	4.4	9.6
A10	7.3	8.7

All splittings are ±0.5 kHz with the exception of MPX-A7d_3 in zwitterionic bicelles, which was given a general value of 0.0 ± 3.0 kHz.
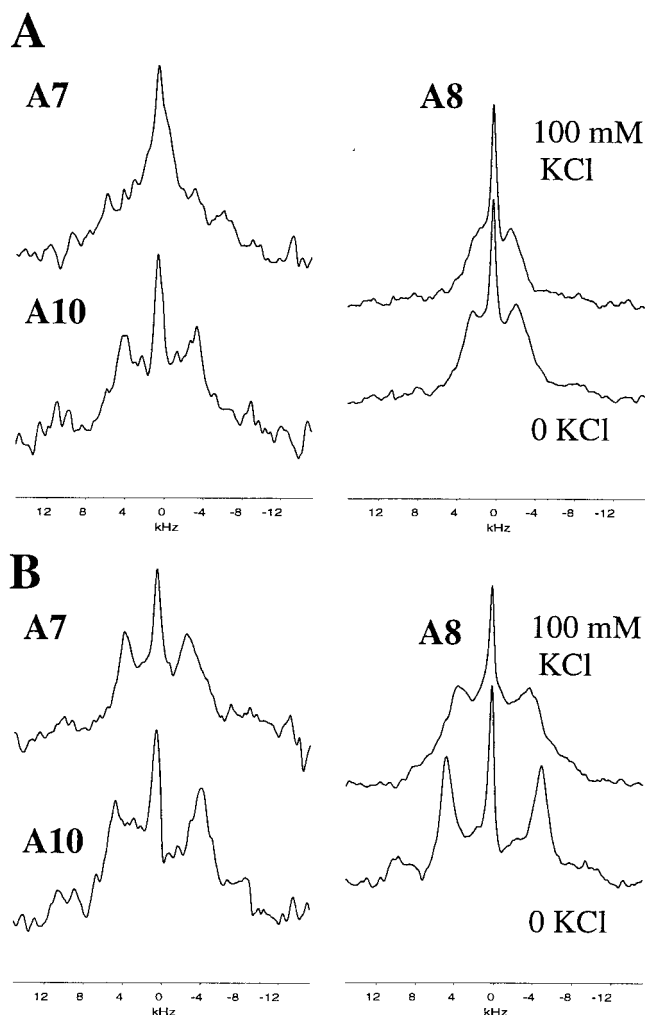
A

A7

A8

100 mM KCl

A10

0 KCl

```
12   8   4   0   -4  -8  -12        12   8   4   0   -4  -8  -12
              kHz                                 kHz
```

B

A7

A8   100 mM KCl

A10

0 KCl

```
12   8   4   0   -4  -8  -12        12   8   4   0   -4  -8  -12
              kHz                                 kHz
```

FIGURE 7   Quadrupolar splitting of MPX-A7d_3, MPX-A8d_3, and MPX-A10d_3 in (A) zwitterionic bicelles (R = 1:40, pH 5.4; and (B) negatively charged bicelles (R = 1:20, pH 5.8. MPX-A8d_3 is shown in the absence and presence of 100 mM KCl. R = ratio of peptide to total long-chain phospholipid. All spectra were recorded at 55.3 MHz and 40°C.

and S^2 are shown in Table 2. For each labeled position, the [^{1}H]-^{15}N NOE ranged from 0.63 to 0.67 in all systems studied, further indicating that MPX bound to bicelles is a well-structured helix, particularly in the regions surrounding our deuterium labels. Although the R_1 values did not vary significantly between residues or for MPX in different bicelle systems, there was a marked increase in R_2 for MPXNB. This may be due to an increased interaction between MPX and the bicelle as a result of an electrostatic attraction between the positively charged peptide side chains and the anionic phosphatidylserine headgroups. The addition of salt to the sample of MPX in negatively charged bicelles (MPXNBKCL) may lead to screening of the electrostatic interaction and result in the observed relaxation data that is similar to that observed for MPXZB.

The generalized order parameter obtained from Model-free analysis of the relaxation data showed that MPX in all systems was well ordered with an S^2 of 0.90 or greater. Others have obtained similarly high values from line-shape analyses for other stable membrane-associated peptides (Koeppe et al., 1994; Prosser et al., 1994). The generalized order parameter, S^2, was reduced to the usual order parameter defined in Eq. 1 (Lipari and Szabo, 1982a) and substituted as S_{pw} in Eq. 10.

Determination of bicelle wobble from ^{2}H NMR

S_{bw} was determined by taking the ratio of the quadrupolar splitting for DMPC-d_{54} in a bicelle to the splitting at the 90° edge of the powder pattern in DMPC-d_{54} MLVs (data not shown). This value was found to be 0.84 ± 0.02 for zwitterionic bicelles and 0.90 ± 0.02 for negatively charged bicelles. These high order parameters indicate bicelles align almost as well as DMPC bilayers aligned on glass plates (Opella and Morden, 1989).

Interaction of MPX with zwitterionic phospholipid bicelles

To examine the effects of MPX on lipid packing and zwitterionic bicelle stability, spectra for both fatty acid perdeuterated DMPC and DHPC in bicelles containing MPX were acquired (Fig. 6). The DHPC-d_{22} spectra were identical in the absence and presence of peptide (R = 1:40), indicating that the bicelles remain stable and well aligned at ratios of MPX to DMPC corresponding to over 100 molecules per bicelle. Because bicelle order is maintained, any perturbations we see in the long-chain lipid spectra in the presence of MPX must result from disruptions in the lipid packing. In the presence of peptide, there were subtle changes in the plateau region of the DMPC-d_{54} whereas the splittings of the remaining methylene and methyl group deuterons (smallest quadrupolar splitting) remained unchanged. These plateau perturbations, which have been seen in other deuterium NMR studies of lipids in the presence of ionophoric peptides, suggest that not only is a significant MPX population associating with the planar region of the bicelle but also that it is interacting near the bilayer interface (Banerjee et al., 1985).

Because the high-resolution NMR experiments indicated that MPX formed a sturdy helix, we were able to use peptides with alanines containing deuterated methyl groups to determine the average angle of orientation for the MPX-d_3 helical axis with respect to the bicelle normal. Deuterium spectra for MPX-A7$_{d3}$, MPX-A8$_{d3}$, and MPX-A10$_{d3}$ were collected for R = 1:40. The observed quadrupolar splittings for these labels are shown in Table 3, and the corresponding spectra are shown in the bottom of Fig. 7 A. Although deuterium-depleted water was used in these ex-
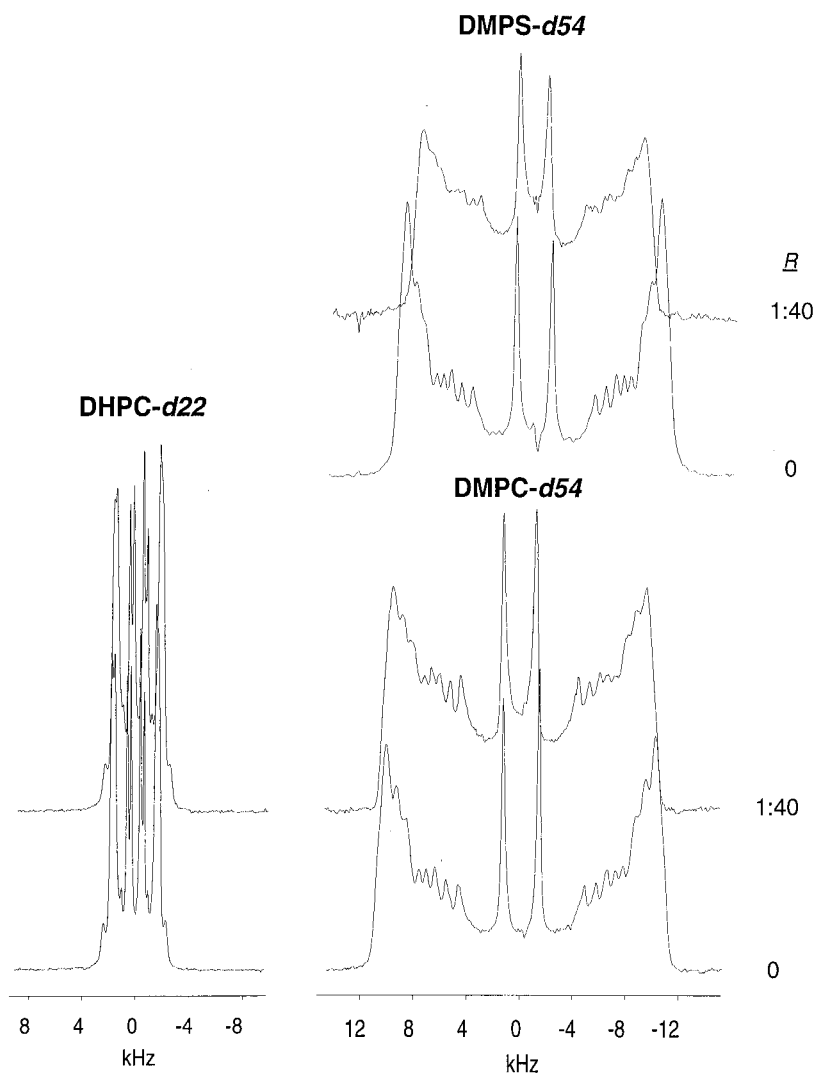
FIGURE 8   Effect of MPX on quadrupolar splittings of perdeuterated phospholipids in negatively charged bicelles. DHPC-d_{22} and DMPC-d_{54} spectra were recorded at 55.3 MHz, and the DMPS-d_{54} spectra were recorded at 38.4 MHz. All spectra were recorded at 40°C and pH 5.8. R = ratio of peptide to total long-chain phospholipid.

periments, control experiments revealed that the sharp peak in the middle of the spectrum resulted from residual heavy water. Other studies have shown that this residual D_2O, or HOD, likely arises from lipid-associated water (Jendrasiak and Hasty, 1974; Struppe et al., 2000). In addition, spectra for MPX-A8$_{d3}$ were collected at various peptide (data not shown) and salt (Fig. 7 A) concentrations. Peptide titrations, ranging from R = 1:40 to 1:20, revealed no significant changes in the observed splitting for MPX-A8$_{d3}$. In addition, the presence of 100 mM KCl (Fig. 7 A) did not have a significant effect on the quadrupolar splitting for MPX-A8$_{d3}$ in zwitterionic bicelles.

Because the quadrupolar splitting of MPX-A7$_{d3}$ was so small that it was not resolvable, we estimated it to be 0.0 kHz with a generous error of ±3.0 kHz. After computational analysis, two possible tilt and rotation combinations were consistent with the quadrupolar splittings for all three deuterium labels, both of which were very similar: 84° tilt with 1°-2° rotation and 75° tilt with 21° rotation. Interpre-

tation of the rotation angles is not possible without a complete understanding of the penetration depth of MPX into the bilayer. Nevertheless, what is most important is that although there are two possible tilt angles, they are both consistent only with MPX resting at a slightly oblique angle nearly parallel to the membrane surface.

Interaction of MPX with negatively charged phospholipid bicelles

Fig. 8 shows lipid spectra for fatty acid perdeuterated DMPC, DMPS, and DHPC in negatively charged bicelles. As in zwitterionic bicelles, the DHPC-d_{22} remained unperturbed by MPX (R = 1:40), indicating that the bicelles remain stable. A comparison of Figs. 6 and 8 shows that MPX was more disruptive to the long-chain lipids in the negatively charged bicelles when compared with the zwitterionic ones. Deuterium labeling of either DMPS or DMPC
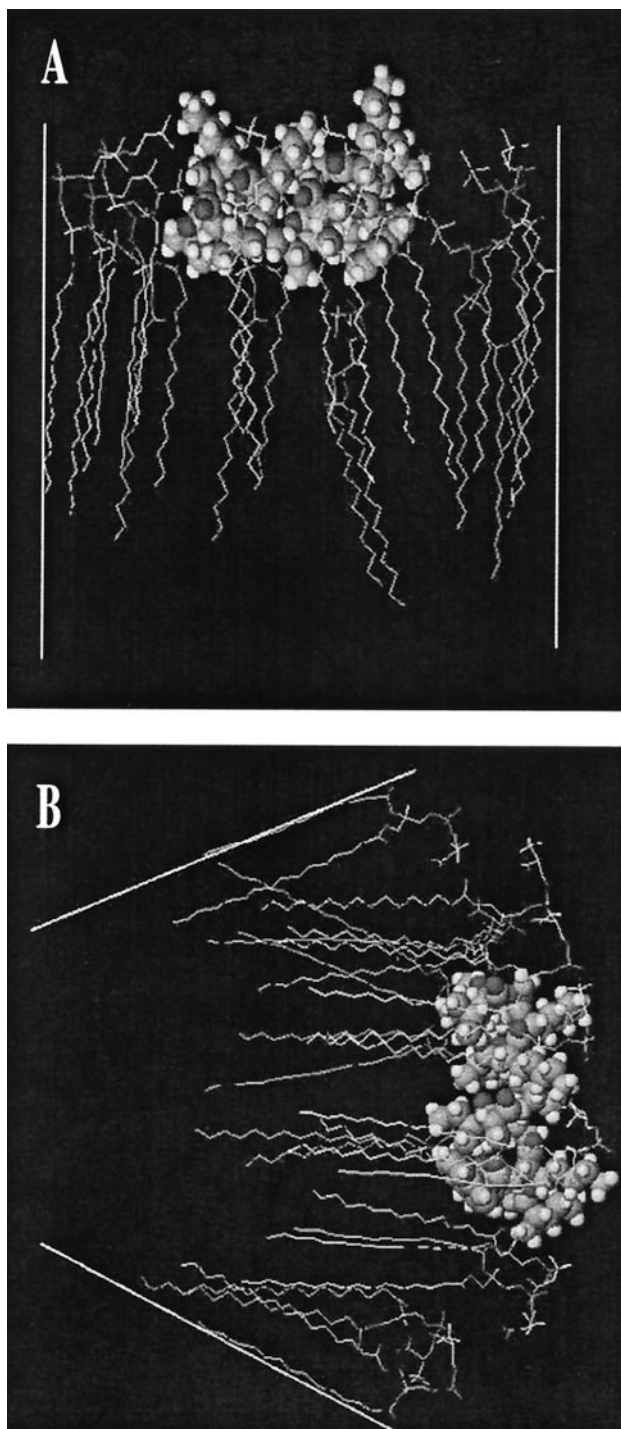
FIGURE 9 Molecular simulations of MPX effects on DMPC (*A*) and DPPS (*B*) at 37°C.

allowed us to individually observe changes in each of the lipids constituting the planar region of the bilayer. There were slight decreases in splitting for the DMPC-d_{54}, plateau and methylene deuterons, whereas the DMPS-d_{54} showed severe distortion throughout the lipid chain. These results imply that not only is MPX interacting with the planar

region of the bicelle (Dufourc et al., 1986), but it is also preferentially interacting with the negatively charged phospholipid. An electrostatic interaction between the positively charged lysine residues and the phosphatidylserine headgroups would facilitate this type of preferential binding. This leads to two interesting possibilities. Either MPX selectively recruits the anionic lipid and induces long-chain lipid segregation or the zwitterionic and the anionic phospholipids are already segregated within the planar region of the bicelle.

The peptide spectra for MPX in negatively charged bicelles are shown in Fig. 7 *B*, and their corresponding quadrupolar splittings are in Table 3. After computer analysis, only one possible tilt and rotation cluster was found: a 17° tilt with a 273°-275° rotation. Again, interpretation of the rotation angle is not possible, but paramount is the striking difference between the tilt angles observed here compared with the results in zwitterionic bicelles. In zwitterionic bicelles, the conclusion was that MPX rested generally parallel to the bicelle surface. Interestingly, the data obtained for MPX in negatively charged bicelles is consistent with a pore-type structure. Simulations of the interaction between DMPC and MPX compared with the interaction between dipalmitoyl phosphatidylserine (DPPS) and MPX show that MPX caused severe positive curvature strain in the negatively charged DPPS but had no such effect on DMPC (Fig. 9). Such curvature of the anionic phospholipids would be expected to result in the disordering of the lipid bilayer, perhaps resulting in porous defects in the bilayer. With the observed angle of MPX being close to perpendicular to the membrane surface, a pore would form in which the anionic phospholipid headgroups line the channel of the pore. In this situation, the molecular axis of the DMPS would no longer be parallel to the bicelle normal. This is consistent with our observation of significantly reduced splittings and large perturbations of only the DMPS-d_{54} in the presence of MPX. This type of channel formation has been suggested previously for MPX (Matsuzaki et al., 1996) as well as other ionophoric peptides such as magainin 2 (Cruciani et al., 1992; Matsuzaki et al., 1998).

As shown in Fig. 7 *B*, the addition of 100 mM KCl lead to a significant decrease in the quadrupolar splitting of MPX-A8d_3 in negatively charged bicelles, and the spectrum was more like that of MPX-A8d_3 in zwitterionic bicelles. The perturbations observed here were too large to be due to salt effects on bicelle stability (Struppe et al., 2000) and are most likely due to electrostatic screening of the peptide-bicelle interaction. In addition, the KCl effects observed in the high-resolution solution NMR support this conclusion.

CONCLUSIONS

The versatility of bicelles coupled with solution-state and solid-state NMR techniques has allowed us to obtain structure, dynamics, and orientation information for MPX bound

to a mimetic membrane as well as the effect of the peptide on lipid order and bicelle stability. We have definitively shown that the orientation of MPX with respect to the bicelle surface is dependent upon the lipid composition and that MPX is more efficient at perturbing the lipid order in negatively charged bicelles. This latter result correlates well with previous studies that showed that MPX induced a higher extent of dye leakage from vesicles doped with anionic lipids (Matsuzaki et al., 1996). Our work suggests that the mode of MPX binding to lipid bilayers, carpet mechanism versus pore formation, is controlled by membrane composition.

REFERENCES

Arbuzova, A., and G. Schwarz. 1996. Pore kinetics of mastoparan peptides in large unilamellar lipid vesicles. *Prog. Colloid. Polymer Sci.* 100: 345–350.

Arbuzova, A., and G. Schwarz. 1999. Pore-forming action of mastoparan peptides on liposomes: a quantitative analysis. *Biochim. Biophys. Acta.* 1420:139–152.

Argiolas, A., and J. J. Pisano. 1983. Facilitation of phospholipase A_2 activity by mastoparans, a new class of mast cell degranulating peptides from wasp venom. *J. Biol. Chem.* 258:13687–13702.

Banerjee, U., R. Zidovetzki, R. R. Birge, and S. I. Chan. 1985. Interaction of alamethicin with lecithin bilayers: a ^{31}P and ^{2}H NMR study. *Biochemistry.* 24:7621–7627.

Bechinger, B., M. Zasloff, and S. J. Opella. 1992. Structure and interactions of magainin antibiotic peptides in lipid bilayers: a solid-state nuclear magnetic resonance investigation. *Biophys. J.* 62:12–14.

Bechinger, B., M. Zasloff, and S. J. Opella. 1998. Structure and dynamics of the antibiotic peptide PGLa in membranes by solution and solid-state nuclear magnetic resonance spectroscopy. *Biophys. J.* 74:981–987.

Bloom, M., E. Evans, and O. G. Mouritsen. 1991. Physical properties of the fluid lipid-bilayer component of cell membranes: a perspective. *Q. Rev. Biophys.* 24:293–297.

Brasseur, R. 1990. Molecular description of biological membrane components by computer aided conformational analysis. CRC Press, Boca Raton, FL.

Brasseur, R. 1991. Differentiation of lipid-associating helices by use of three-dimensional molecular hydrophobicity potential calculations. *J. Biol. Chem.* 266:16120–16127.

Brasseur, R., J. A. Killian, B. De Kruijff, and J. M. Ruysschaert. 1987. Conformational analysis of gramicidin-gramicidin interactions at the air/water interface suggests that gramicidin aggregates into tube-like structures similar as found in the gramicidin-induced hexagonal HII phase. *Biochim. Biophys. Acta.* 903:11–17.

Brasseur, R., L. Lins, B. Vanloo, J. M. Ruysschaert, and M. Rosseneu. 1992. Molecular modeling of the amphipathic helices of the plasma apolipoproteins. *Proteins.* 13:246–257.

Cross, T. A., and S. J. Opella. 1994. Solid-state NMR structural studies of peptides and proteins in membranes. *Curr. Opin. Struct. Biol.* 4:574–581.

Cruciani, R. A., J. L. Barker, S. R. Durell, G. Raghunathan, H. R. Guy, M. Zasloff, and E. F. Stanley. 1992. Magainin 2, a natural antibiotic from frog skin, forms ion channels in lipid bilayer membranes. *Eur. J. Pharmacol.* 226:287–296.

Davis, J. H. 1983. The description of membrane lipid conformation, order, and dynamics by ^{2}H-NMR. *Biochim. Biophys. Acta.* 737:117–171.

Davis, J. H., K. R. Jeffrey, M. Bloom, M. I. Valic, and T. P. Higgs. 1976. Quadrupolar echo deuteron magnetic resonance spectroscopy in ordered hydrocarbon chains. *Chem. Phys. Lett.* 42:390.

de Kroon, A., de Gier, J., and B. de Kruijff. 1991. The effect of a membrane potential on the interaction of mastoparan X, a mitochondrial presequence, and several regulatory peptides with phospholipid vesicles. *Biochim. Biophys. Acta.* 1068:111–124.

Dufourc, E. J., I. C. P. Smith, and J. Dufourcq. 1986. Molecular details of melittin-induced lysis of phospholipid membranes as revealed by deuterium NMR and phosphorus NMR. *Biochemistry.* 25:6448–6455.

Edelhoch, H. 1967. Spectroscopic determination of tryptophan and tyrosine in proteins. *Biochemistry.* 6:1948–1954.

Epand, R. M., Y. Shai, J. P. Segrest, and G. M. Anantharamaiah. 1995. Mechanisms for the modulation of membrane bilayer properties by amphipathic helical peptides. *Biopolymers Peptide Sci.* 37:319–338.

Farrow, N. A., R. Muhandiram, A. V. Singer, S. M. Pascal, C. M. Kay, G. Gish, S. E. Shoelson, T. Pawson, J. D. Forman-Kay, and L. E. Kay. 1994. Backbone dynamics of a free and phosphopeptide-complexed Src homology 2 domain studied by ^{15}N NMR relaxation. *Biochemistry.* 33:5984–6003.

Fujita, K., K. Shunsaku, and Y. Imanishi. 1994. Self-assembly of mastoparan X derivative having fluorescence probe in lipid bilayer membrane. *Biochim. Biophys. Acta.* 1195:157–163.

Hellmann, N., and G. Schwarz. 1998. Peptide-liposome association: a critical examination with mastoparan-X. *Biochim. Biophys. Acta.* 1369: 267–277.

Higashijima, T., S. Uzu, T. Nakajima, and E. M. Ross. 1988. Mastoparan, a peptide from toxin from wasp venom, mimics receptors by activating GTP-binding regulatory proteins (G proteins). *J. Biol. Chem.* 263: 6491–6494.

Higashijima, T., K. Wakamatsu, S. Kazuki, F. Masahiko, T. Nakajima, and T. Miyazawa. 1984. Molecular aggregation and conformational change of wasp venom mastoparan as induced by salt in aqueous solution. *Biochim. Biophys. Acta.* 802:157–161.

Higashijima, T., K. Wakamatsu, M. Takemitsu, M. Fujino, T. Nakajima, and T. Miyazawa. 1983. Conformational change of mastoparan from wasp venom on binding with phospholipid membrane. *FEBS Lett.* 152: 227–230.

Howard, K. P., and S. J. Opella. 1996. High resolution solid-state NMR spectra of integral membrane proteins reconstituted into magnetically oriented phospholipid bilayers. *J. Magn. Reson.* 112:91–94.

Jendrasiak, G. L., and J. H. Hasty. 1974. The hydration of phospholipids. *Biochim. Biophys. Acta.* 337:79–91.

Jones, D. H., K. R. Barber, E. W. VanDerLoo, and C. W. M. Grant. 1998. Epidermal growth factor receptor transmembrane domain: ^{2}H NMR implications for orientation and motion in a bilayer environment. *Biochemistry.* 37:16780–16787.

Koeppe, R. E. II, J. A. Killian, and D. V. Greathouse. 1994. Orientations of the tryptophan 9 and 11 side chains of the gramicidin channel based on deuterium nuclear magnetic resonance spectroscopy. *Biophys. J.* 66:14–24.

Kovacs, F. A., and T. A. Cross. 1997. Transmembrane four-helix bundle of influenza A M2 protein channel: structural implications from helix tilt and orientation. *Biophys. J.* 73:2511–2517.

Kuntz, I. D., P. A. Kosen, and E. C. Craig. 1991. Amide chemical shifts in many helices in peptides and proteins are periodic. *J. Am. Chem. Soc.* 113:1406–1408.

Kusunoki, H., K. Wakamatsu, K. Sato, T. Miyazawa, and T. Kohno. 1998. G protein-bound conformation of mastoparan-X: heteronuclear multidimensional transferred nuclear overhauser effect analysis of peptide uniformly enriched with ^{13}C and ^{15}N. *Biochemistry.* 37:4782–4790.

Lins, L., and R. Brasseur. 1995. The hydrophobic effect in protein folding. *FASEB J.* 9:535–540.

Lipari, G., and A. Szabo. 1982a. Model-free approach to the interpretation of nuclear magnetic resonance relaxation in macromolecules. I. Theory and range of validity. *J. Am. Chem. Soc.* 104:4546–4559.

Lipari, G., and A. Szabo. 1982b. Model-free approach to the interpretation of nuclear magnetic resonance relaxation in macromolecules. II. Analysis of experimental results. *J. Am. Chem. Soc.* 104:4559–4570.

Losonczi, J. A., and J. H. Prestegard. 1998. Nuclear magnetic resonance characterization of the myristoylated, N-terminal fragment of ADP-ribosylation factor 1 in a magnetically oriented membrane array. *Biochemistry.* 37:706–716.

Malencik, D. A., and S. R. Anderson. 1983. High affinity binding of the mastoparans by calmodulin. *Biochem. Biophys. Res. Commun.* 114:50–56.

Marion, D., and K. Wüthrich. 1983. Application of phase sensitive two-dimensional correlated spectroscopy (COSY) for measurements of ^{1}H-^{1}H spin-spin coupling constants in proteins. *Biochem. Biophys. Res. Commun.* 113:967–974.

Matsuzaki, K., K. Sugishita, M. Ueha, S. Nakata, K. Miyajima, and R. M. Epand. 1998. Relationship of membrane curvature to the formation of pores by magainin 2. *Biochemistry.* 37:11856–11863.

Matsuzaki, K., S. Yoneyama, M. Osamu, and K. Miyajima. 1996. Transbilayer Transport of ions and lipids coupled with mastoparanx X translocation. *Biochemistry.* 35:8450–8456.

Mellor, I. R., and M. S. P. Sansom. 1990. Ion-channel properties of mastoparan, a 14-residue peptide from wasp venom, and of MP3, a 12-residue analogue. *Proc. R. Soc. Lond.* 239:383–400.

Nelder, J. A., and R. A. Mean. 1965. A simplex method for function minimization. *Comput. J.* 7:308–313.

North, C. L., M. Barranger-Mathys, and D. S. Cafiso. 1995. Membrane orientation of the N-terminal segment of alamethicin determined by solid-state ^{15}N NMR. *Biophys. J.* 69:2392–2397.

Okamura, K., K. Inui, Y. Hirai, and T. Nakajima. 1981. The effect of mastoparan on movement in black lipid membrane. *Biomed. Res.* 2:450–452.

Opella, S. J., and K. M. Morden. 1989. ^{15}N NMR-spectroscopy of DNA in the solid state. *In* Dynamic Properties of Biomolecular Assemblies. C. S. E. Harding and A. J. Rowe, editors. The Royal Society of Chemistry, Cambridge, UK. 196.

Palmer, A. G. 1998. Curvefit. University of Columbia, New York, NY.

Palmer, A. G. 1998. Modelfree. University of Columbia, New York, NY.

Piotto, M., V. Saudek, and V. Sklenar. 1992. Gradient-tailored excitation for single-quantum NMR spectroscopy of aqueous solutions. *J. Biomol. NMR.* 2:661–665.

Prosser, R. S., S. I. Daleman, and J. H. Davis. 1994. The structure of an integral membrane peptide: a deuterium NMR study of gramicidin. *Biophys. J.* 66:1415–1428.

Prosser, S. R., J. S. Hwang, and R. R. Vold. 1998. Magnetically aligned phospholipid bilayers with positive ordering: a new model membrane system. *Biophys. J.* 74:2405–2418.

Ram, P., and J. H. Prestegard. 1988. Magnetic field induced ordering of bile salt/phospholipid micelles: new media for NMR structural investigations. *Biochim. Biophys. Acta.* 940:289–294.

Reymond, M. T., S. Huo, B. Duggan, P. E. Wright, and J. H. Dyson. 1997. Contribution of increased length and intact capping sequences to the conformational preference for helix in a 31-residue peptide from the C-terminus of myohymorethrin. *Biochemistry.* 36:5234–5244.

Sanders, C. R., B. J. Hare, K. P. Howard, and J. H. Prestegard. 1994. Magnetically oriented phospholipid micelles as a tool for the study of membrane associated molecules. *Prog. NMR Spectrosc.* 26:421–444.

Sanders, C. R., and G. C. Landis. 1995. Reconstitution of membrane proteins into lipid-rich bilayered mixed micelles for NMR studies. *Biochemistry.* 43:4030–4040.

Sanders, C. R., and J. H. Prestegard. 1990. Magnetically orientable phospholipid bilayers containing small amounts of a bile salt analogue, CHAPSO. *Biophys. J.* 58:447–460.

Sanders, C. R., and J. P. Schwonek. 1992. Characterization of magnetically orientable bilayers in mixtures of dihexanoylphosphatidylcholine and dimyristoylphosphatidylcholine by solid-state NMR. *Biochemistry.* 31:8898–8905.

Schwarz, G., and U. Blochmann. 1993. Association of the wasp venom peptide mastoparan with electrically neutral lipid vessicles. *FEBS Lett.* 318:172–176.

Seelig, J. 1977. Deuterium magnetic resonance: theory and application to lipid membranes. *Q. Rev. Biophys.* 10:353–418.

Seigneuret, M., and D. Levy. 1995. A high-resolution ^{1}H approach for structure determination of membrane peptides and proteins in non-deuterated detergent: application to mastoparan X solubilized in *n*-octylglucoside. *J. Biomol. NMR.* 5:345–352.

Struppe, J. O. F., E. A. Komives, S. S. Taylor, and R. R. Vold. 1998. ^{2}H NMR studies of a myristoylated peptide in neutral and acidic phospholipid bicelles. *Biochemistry.* 37:15523–15527.

Struppe, J. O., J. A. Whiles, and R. R. Vold. 2000. Acidic phospholipid bicelles: a versatile model membrane system. *Biophys. J.* 78:281–289.

Szilagyi, L., and O. Jardetzky. 1989. α-Proton chemical shifts and secondary structure in proteins. *J. Magn. Reson.* 83:441–449.

van Tilborg, P. J. A., F. A. A. Mulder, M. M. E. de Backer, M. Nair, E. C. van Heerde, G. Folkers, P. T. van der Saag, Y. Karimi-Nejad, R. Boelens, and R. Kaptein. 1999. Millisecond to microsecond time scale dynamics of the retinoid X and retinoic acid receptor DNA-binding domains and dimeric complex formation. *Biochemistry.* 38:1951–1956.

Vold, R. R., and R. S. Prosser. 1996. Magnetically oriented phospholipid bilayered micelles for structural studies of polypeptides: does the ideal bicelle exist? *J. Magn. Reson. B.* 113:267–271.

Vold, R. R., R. S. Prosser, and A. J. Deese. 1997. Isotropic solutions of phospholipid bicelles: a new membrane mimetic for high-resolution NMR studies of polypeptides. *J. Biomol. NMR.* 9:329–335.

Wakamatsu, K., A. Okada, T. Miyazawa, M. Ohya, and T. Higashijima. 1992. Membrane-bound conformation of mastoparan-X, a G-protein-activating peptide. *Biochemistry.* 31:5654–5660.

Wishart, D. S., C. G. Bigam, J. Yao, F. Abildgaard, H. J. Dyson, E. Oldfield, J. L. Markley, and B. D. Sykes. 1995. ^{1}H, ^{13}C and ^{15}N chemical shift referencing in biomolecular NMR. *J. Biomol. NMR.* 6:135–140.

Wüthrich, K. 1986. NMR of Proteins and Nucleic Acids. John Wiley and Sons, New York.

Zhou, N. E., B.-Y. Zhu, B. D. Sykes, and R. S. Hodges. 1992. Relationship between amide proton chemical shifts and hydrogen bonding on amphipathic α-helical peptides. *J. Am. Chem. Soc.* 114:4320–4326.